

## Electronic Supplementary Information

# Dispersion-controlled docking preference: multi-spectroscopic study on complexes of dibenzofuran with alcohols and water

D. Bernhard<sup>a</sup>, M. Fatima<sup>b</sup>, A. Poblotzki<sup>c</sup>, A. L. Steber<sup>b</sup>, C. Pérez<sup>b</sup>,  
M. A. Suhm<sup>\*c</sup>, M. Schnell<sup>\*b</sup>, M. Gerhards<sup>\*a</sup>

<sup>a</sup>Fachbereich Chemie & Research Center Optimas, Technische Universität Kaiserslautern,  
Erwin-Schrödinger Str. 52, D-67663 Kaiserslautern

<sup>b</sup>Deutsches Elektronen-Synchrotron (DESY), Notkestrasse 85, D-22607 Hamburg &  
Institute of Physical Chemistry, Christian-Albrechts-Universität zu Kiel, Max-Eyth-Strasse 1, D-24118 Kiel

<sup>c</sup>Institut für Physikalische Chemie, Georg-August-Universität Göttingen, Tammannstrasse 6, D-37077 Göttingen

**Table S1:** Different contributions to the total interaction energy obtained at the SAPT(0)/jun-cc-pVDZ results for different DBF–ROH complexes. All values are given in kJ/mol.

contribution	DBF–H <sub>2</sub> O			DBF–MeOH			DBF–t-BuOH		
	OH···Op	OH···π5	OH···π6	OH···Ot	OH···Op	OH···π6	OH···Ot	OH···Op	OH···π6
$E_{\text{elst}}$	-27.94	-16.75	-13.84	-22.24	-28.54	-15.92	-22.60	-26.25	-16.05
$E_{\text{exch}}$	25.73	20.50	18.37	26.42	28.43	23.97	35.60	35.05	29.19
$E_{\text{ind}}$	-7.00	-4.51	-4.27	-5.81	-7.09	-5.00	-6.80	-7.35	-5.57
$E_{\text{disp}}$	-9.38	-12.16	-11.91	-19.15	-14.27	-21.70	-31.53	-27.95	-31.04
$E_{\text{tot}}$	-18.59	-12.92	-11.65	-20.78	-21.47	-18.65	-25.34	-26.50	-23.47

**Table S2:** Dispersion energy contributions to the total interaction energy obtained at the DLPNO-CCSD(T)/cc-pVQZ level via a local decomposition (LED) scheme for different DBF–ROH complexes. All values are given in kJ/mol.

	DBF–H <sub>2</sub> O			DBF–MeOH			DBF–t-BuOH		
	OH···Op	OH···π5	OH···π6	OH···Ot	OH···Op	OH···π6	OH···Ot	OH···Op	OH···π6
$E_{\text{disp}}$	-8.06	-9.78	-8.81	-16.26	-12.37	-18.17	-23.63	-21.46	-23.45

**Table S3:** Structural parameters for different OH···O structures of DBF–ROH complexes.

	DBF–H <sub>2</sub> O		DBF–MeOH		DBF–tBuOH	
	OH···Op	OH···Ot	OH···Op	OH···Ot	OH···Op	
<b>α(O-H···O) / °</b>						
B3LYP-D3(BJ)/def2-TZVP	160		155	155	177	164
B3LYP-D3(BJ)/aug-cc-pVTZ	161		153	157	178	163
<b>r(O-H) / Å</b>						
B3LYP-D3(BJ)/def2-TZVP	0.967		0.965	0.965	0.965	0.966
B3LYP-D3(BJ)/aug-cc-pVTZ	0.967		0.963	0.964	0.964	0.965
<b>r(OH···O) / Å</b>						
B3LYP-D3(BJ)/def2-TZVP	2.026		2.068	2.034	2.108	2.042
B3LYP-D3(BJ)/aug-cc-pVTZ	2.009		2.068	2.030	2.122	2.044
<b>r(CH···O) / Å</b>						
B3LYP-D3(BJ)/def2-TZVP	2.733		–	2.659	–	3.237
B3LYP-D3(BJ)/aug-cc-pVTZ	2.716		–	2.762	–	3.204

**Table S4:** Relative energies of DBF–ROH complexes (R= H, Me, *t*-Bu) calculated at different theoretical levels. All values have been corrected for the BSSE, except for the DLPNO-CCSD(T) calculations. The DLPNO-CCSD(T) energies have been augmented by the respective ZPE obtained at the B3LYP-D3(BJ)/aug-cc-pVTZ level. All values are given in kJ/mol.

method	$\Delta E$	DBF–H <sub>2</sub> O			DBF–MeOH			DBF– <i>t</i> -BuOH		
		OH···Op	OH···π5	OH···π6	OH···Ot	OH···Op	OH···π6	OH···Ot	OH···Op	
B3LYP-D3(BJ)/	$\Delta E$	<b>0</b>	2.42	3.79	1.33	<b>0</b>	1.22	<b>0</b>	1.66	2.35
def2-TZVP	$\Delta E_0$	<b>0</b>	1.18	1.47	0.96	0.57	<b>0</b>	<b>0</b>	1.57	1.29
B3LYP-D3(BJ)/	$\Delta E$	<b>0</b>	2.92	3.87	<b>0</b>	0.39	0.03	0.16	<b>0</b>	0.78
aug-cc-pVTZ	$\Delta E_0$	<b>0</b>	1.88	2.02	0.05	1.06	<b>0</b>	0.84	0.21	<b>0</b>
B3LYP-D3(BJ)/	$\Delta E$	<b>0</b>	2.92	4.03	<b>0</b>	0.23	0.09	0.26	<b>0</b>	0.86
def2-QZVP	$\Delta E_0$	<b>0</b>	1.50	1.57	0.54	1.18	<b>0</b>	0.59	0.65	<b>0</b>
M06-2X/	$\Delta E$	<b>0</b>	0.45	1.27	1.08	1.02	<b>0</b>	2.42	1.10	<b>0</b>
def2-TZVP	$\Delta E_0$	0.81	<b>0</b>	0.24	1.40	2.54	<b>0</b>	2.91	2.57	<b>0</b>
SCS-CC2/	$\Delta E$	<b>0</b>	1.17	-	1.99	-	<b>0</b>	1.65	-	<b>0</b>
aug-cc-pVDZ	$\Delta E_0$	0.76	<b>0</b>	-	3.63	-	<b>0</b>	2.07	-	<b>0</b>
SCS-CC2/	$\Delta E$	<b>0</b>	0.58	-	0.88	1.62	<b>0</b>	0.64	0.60	<b>0</b>
def2-TZVP	$\Delta E_0$	1.58	<b>0</b>	-	1.88	3.63	<b>0</b>	0.85	1.38	<b>0</b>
DLPNO-CCSD(T)/	$\Delta E$	<b>0</b>	3.60	4.65	1.71	<b>0</b>	2.71	1.43	<b>0</b>	2.35
cc-pVTZ	$\Delta E_0$	<b>0</b>	2.56	2.79	1.08	<b>0</b>	2.00	0.54	1.39	<b>0</b>
DLPNO-CCSD(T)/	$\Delta E$	<b>0</b>	3.38	3.80	0.85	<b>0</b>	1.21	0.98	<b>0</b>	1.48
cc-pVQZ	$\Delta E_0$	<b>0</b>	2.34	1.95	0.21	<b>0</b>	0.51	1.46	<b>0</b>	0.49

**Table S5:** Comparison of calculated and experimental shifts of  $S_1 \leftarrow S_0$  excitation energies for the DBF–ROH complexes with respect to the DBF monomer transition at  $33657\text{ cm}^{-1}$ . All values are given in  $\text{cm}^{-1}$ . Values in parentheses are calculated oscillator strengths for the respective electronic transition.

H <sub>2</sub> O			MeOH			t-BuOH			
	OH···Op	OH···π5	OH···π6	OH···Ot	OH···π6	OH···Op	OH···Ot	OH···π6	OH···Op
SCS-CC2/ def2-TZVP	<b>+174</b> (0.02933)	+1168 (0.29596)	-138*	<b>+126</b> (0.02174)	<b>-245</b> (0.04386)	+1523 (0.28563)	+98 (0.02100)	<b>-263</b> (0.03730)	+1585 (0.26715)
experiment	<b>+171</b>			<b>+135</b>	<b>-24</b>			<b>-39</b>	

\* only obtained with basis set aug-cc-pVDZ

**Table S6:** Harmonic OH stretching wavenumbers  $\tilde{\nu}_{\text{OH}}$  for DBF–ROH complexes obtained at different levels of theory. Scaling factors (*cf.* Table S3) obtained from reference calculations of the free solvent molecule, respectively.  $\tilde{\nu}_{\text{OH},\text{sym}}$  is used for DBF–H<sub>2</sub>O. The bold values indicate an inverse frequency order for OH···Ot and OH···π6.

method	DBF–H <sub>2</sub> O						DBF–MeOH				DBF–t-BuOH	
	OH···Op	OH···π5	OH···π6	OH···Ot	OH···Op	OH···π6	OH···Ot	OH···Op	OH···π6	OH···Ot	OH···Op	OH···π6
B3LYP- D3(BJ)/ def2-TZVP	3623	3735	3651	3735	3653	3739	3649	3639	3660	3579	3604	3624
B3LYP- D3(BJ)/ aug-cc-pVTZ	3604	3735	3645	3728	3638	3737	3655	3630	3664	3616	3629	3638
B3LYP- D3(BJ)/ def2-QZVP	3631	3758	3670	3754	3662	3762	3648	3636	3658	3617	3603	3622
M06-2X/ def2-TZVP	3624	3728	3634	3720	3636	3722	<b>3662</b>	3655	<b>3652</b>	<b>3627</b>	3613	<b>3617</b>
SCS-CC2/ aug-cc- pVDZ	3617	3756	3634	3744	-	-	<b>3654</b>	-	<b>3649</b>	<b>3628</b>	-	<b>3616</b>
SCS-CC2/ def2-TZVP	3630	3747	3634	3740	-	-	<b>3658</b>	3653	<b>3657</b>	<b>3627</b>	3614	<b>3622</b>

**Table S7:** Scaling factors for different computational approaches obtained from reference calculations for the free solvent molecule, respectively.

	DBF-H <sub>2</sub> O	DBF-MeOH	DBF- <i>t</i> -BuOH
B3LYP-D3(BJ)/ def2-TZVP	0.9677	0.9674	0.9618
B3LYP-D3(BJ)/ aug-cc-pVTZ	0.9646	0.9633	0.9596
B3LYP-D3(BJ)/ def2-QZVP	0.9677	0.9616	0.9563
M06-2X/ def2-TZVP	0.9464	0.9480	0.9449
SCS-CC2/ aug-cc-pVDZ	0.9704	0.9684	0.9681
SCS-CC2/ def2-TZVP	0.9668	0.9681	0.9686

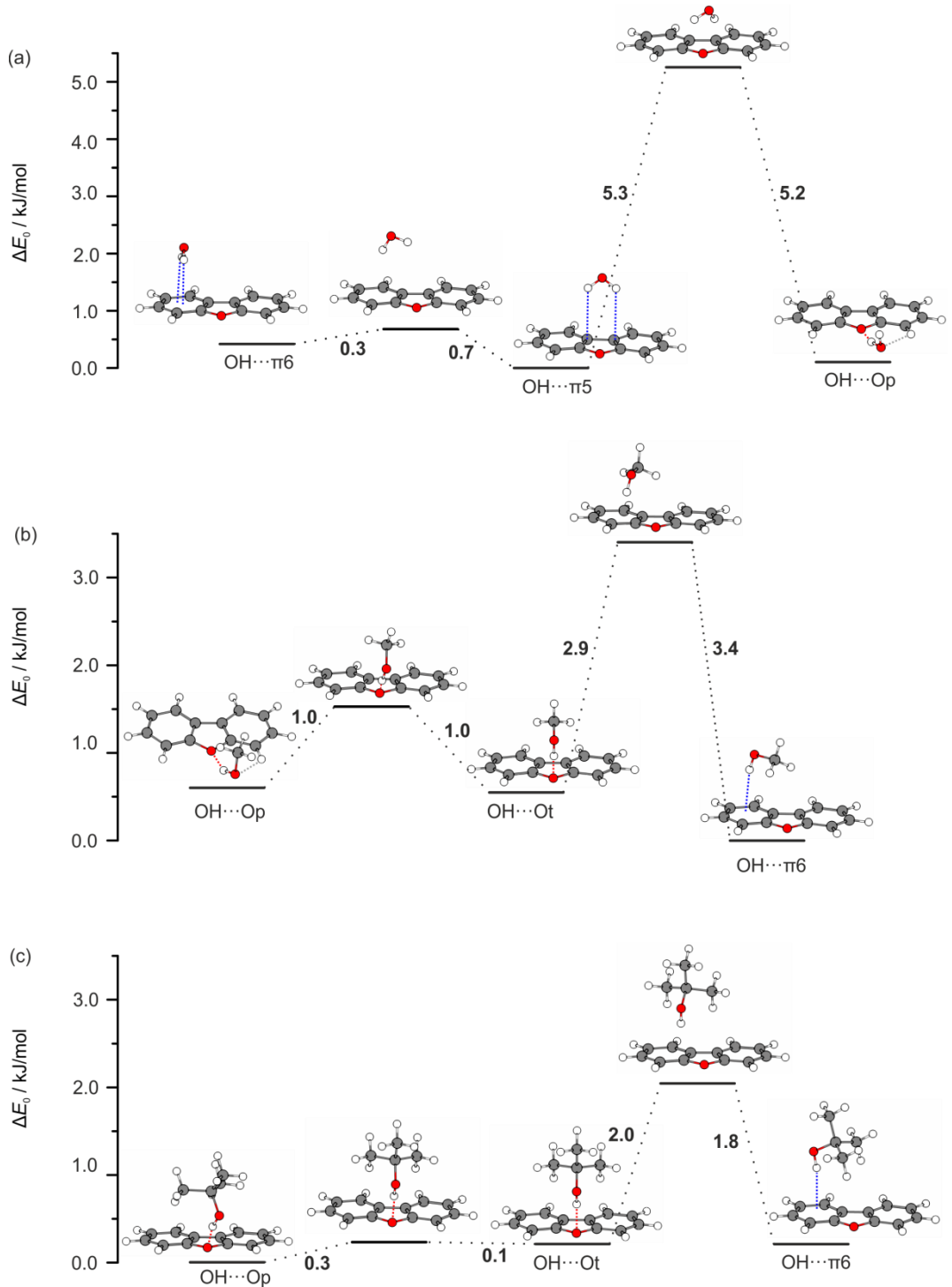


**Fig. S1:** Isomer interconversion barriers obtained at the B3LYP-D3(BJ)/def2-TZVP level (QST3 method within Gaussian 09).

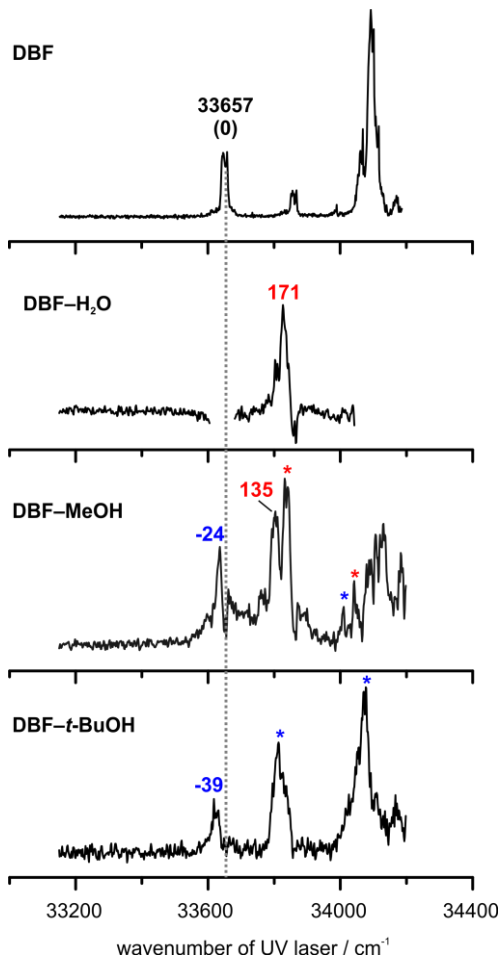


**Fig. S2:** R2PI spectra of different DBF-ROH complexes. Asterisks mark additional vibronic transitions yielding the same IR/R2PI spectra as the ones that are labeled with numbers. Blue labels mark OH $\cdots$  $\pi$  transitions whereas red transitions mark OH $\cdots$ O transitions. The gaps in the DBF-H<sub>2</sub>O spectrum are at positions of strong monomer transitions influencing the DBF-H<sub>2</sub>O trace involving a weak ion signal. The dip in the DBF-MeOH spectrum at the monomer transition indicates an influence of the much larger monomer signal as well and therefore distorts relative intensities. The intense electronic origin of the monomer is so close to the OH $\cdots$  $\pi$ 6 transition of DBF-MeOH ( $-24\text{ cm}^{-1}$ ) that it reduces its actual intensity within a range of about  $\pm 30\text{ cm}^{-1}$  around the monomer transition (grey dotted line in Fig. S2). On the other hand, the transition of the OH $\cdots$ O<sub>t</sub> structure at  $+135\text{ cm}^{-1}$  is almost unaffected by the monomer as there is no close monomer transition. Moreover, the OH $\cdots$  $\pi$ 6 transition is “contaminated” by fragmentation of larger clusters (*cf.* Fig. S3, ESI), which is reflected in the corresponding IR/R2PI spectrum (*cf.* Fig. 4b). In contrast, the OH $\cdots$ O<sub>t</sub> transition is not influenced by fragmentation indicated by its clean IR/R2PI spectrum (*cf.* Fig. 4a). Altogether, the relative peak intensities within the R2PI spectrum and thus the estimation of relative populations of the OH $\cdots$  $\pi$ 6 and the OH $\cdots$ O<sub>t</sub> isomers are largely uncertain.

#### Remark on relative shifts in the R2PI spectrum:

It has been shown in several examples (*cf. e.g.* DOI: 10.1021/acs.chemrev.5b00652 and Refs. therein) that  $\pi$ -bound complexes exhibit a red-shifted electronic resonance compared to the monomer, since their binding energy is larger in the  $S_1$  compared to the  $S_0$  state. This can be rationalized by a slightly increased electron density of the  $\pi$ -cloud accompanying the  $\pi - \pi^*$  transition, as electron density is removed from the DBF oxygen atom. This allows for stronger interactions involving the  $\pi$  cloud leading to a larger binding energy of the complex than in the ground state. In contrast, the OH $\cdots$ O-bound complexes are destabilized in the  $S_1$  state, as the electron density at the DBF oxygen atom is reduced, yielding a worse H-bond acceptor compared to the  $S_0$  state. This on the other hand causes a blue-shifted electronic transition compared to the ground state. Table S5 suggests that these blue-shifts are predicted quite closely by theory, whereas the red-shifts are predicted qualitatively.

### Comparison to related systems:

#### **DBF–H<sub>2</sub>O**

A comparison of the IR/UV results to the ones for the related 2,3-benzofuran–H<sub>2</sub>O complex by Sasaki *et al.*<sup>1</sup> is interesting: they found two co-existing isomers identified as an OH···O and an OH···π isomer with pairs of OH stretching frequencies at 3625 and 3736 cm<sup>-1</sup> as well as 3633 and 3740 cm<sup>-1</sup>, respectively. Remarkably, upon comparison to the herein investigated DBF–H<sub>2</sub>O complex, the frequencies for the OH···O isomer are identical (within 2 cm<sup>-1</sup>) to the ones observed in our experiment, which we assigned to the OH···Op complex. This suggests that a second benzene ring attached to benzofuran does not affect the furan oxygen docking site, providing an identical environment for the attached H<sub>2</sub>O molecule in both 2,3-benzofuran and dibenzofuran. Interestingly, the π acceptor site seems to be less attractive in DBF compared to 2,3-benzofuran, as no π-bound structure is observed for DBF–H<sub>2</sub>O, but it is found for 2,3-benzofuran–H<sub>2</sub>O. The predicted energetic disadvantage of ≈2 kJ/mol for OH···π<sup>5</sup> at the highest applied level of theory is in line with the experiment, as only the OH···Op structure is observed. However, it should be noted that Sasaki *et al.* performed their experiments in helium expansion whereas neon has been used within the presented work, certainly influencing the isomer population.

#### **DBF–MeOH**

It is known *e.g.* from investigations on 1-indanol<sup>2</sup> or benzyl alcohol and other systems<sup>3</sup> that the OH stretching shifts compared to free MeOH calculated at the B3LYP-D3 level are usually overestimated for OH···O-bound structures and underestimated for OH···π-bound structures. This even led to a switched order of OH stretching frequencies for OH···O and OH···π isomers in the very closely related case of 2,3-benzofuran–MeOH studied by FTIR jet spectroscopy<sup>4</sup>, and by IR/UV spectroscopy<sup>1</sup>. For 2,3-benzofuran–MeOH, two isomers were found with OH stretching vibrations at 3636 and 3645 cm<sup>-1</sup> respectively<sup>4</sup>, which are remarkably similar to the frequencies found in the presented experiments on DBF–MeOH (*cf.* Fig. 3 and 4). Calculations at the B3LYP/6-311++G(d,p) and B3LYP-D3(BJ)/aug-cc-pVTZ level suggested the OH···O structure to show the larger OH stretching red-shift, whereas the functional M05-2X as well as MP2 calculations, both using the 6-311++G(d,p) basis set, predicted a reverse order. By analyzing the intermolecular modes<sup>1</sup> and by performing experiments with MeOD instead of MeOH<sup>4</sup>, the less shifted band could be clearly assigned to the weakly populated OH···O isomer, confirming the π cloud to be the stronger hydrogen bond acceptor site. Consequently, the frequency shifts were predicted wrongly using the B3LYP functional (independent on the use of dispersion corrections), whereas the M05-2X functional as well as MP2 predicted the right order of shifts. Building on these findings for the very related system of 2,3-benzofuran, the similarity of a different OH stretching frequency order predicted by B3LYP-D3(BJ) calculations than for other approaches is obvious. The M06-2X functional is known to perform worse than B3LYP-D3(BJ) for predicting the energetic order of such intermolecular energy balances as it exhibits a systematic bias towards π-bound structures.<sup>5</sup> Nevertheless, this does not necessarily affect the performance of vibrational frequency predictions. Therefore, based on the intriguing analogy to the 2,3-benzofuran–methanol complex, the frequency order obtained by M06-2X/def2-TZVP and the SCS-CC2 calculations is regarded as the most probable one. Hence, the transition at 3642 cm<sup>-1</sup> is assigned to the OH···Ot structure, whereas the transition at 3637 cm<sup>-1</sup> is assigned to the OH···π<sup>6</sup> isomer.

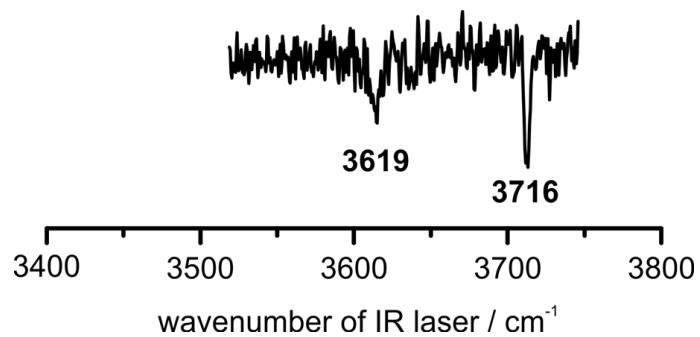


**Fig. S3:** IR/R2PI spectrum of DBF–MeOH–H<sub>2</sub>O, carrier gas neon.

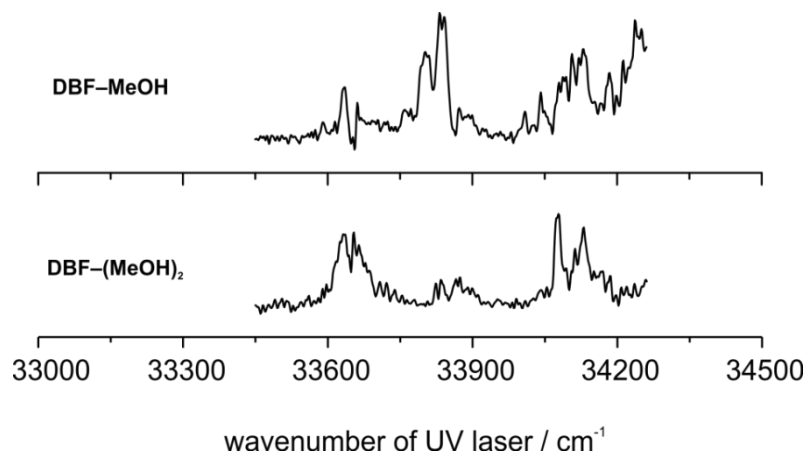


**Fig. S4:** R2PI spectra of the DBF–MeOH and DBF–(MeOH)<sub>2</sub> mass traces for the carrier gas neon.

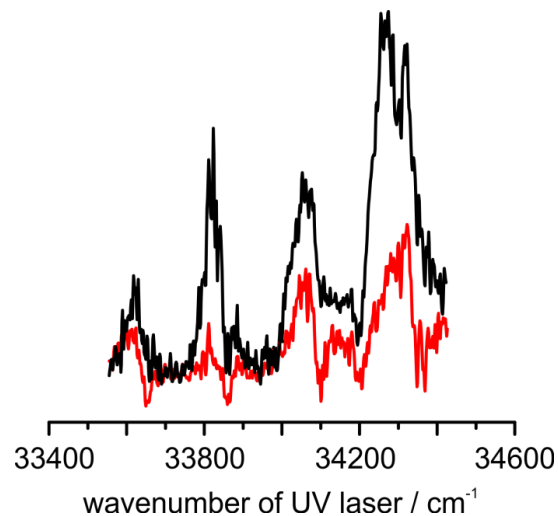


**Fig. S5:** IR(fixed)/R2PI spectrum (red trace) of the DBF–t–BuOH with IR burn laser fixed on 3605 cm<sup>-1</sup>, compared to the original R2PI spectrum (black trace).

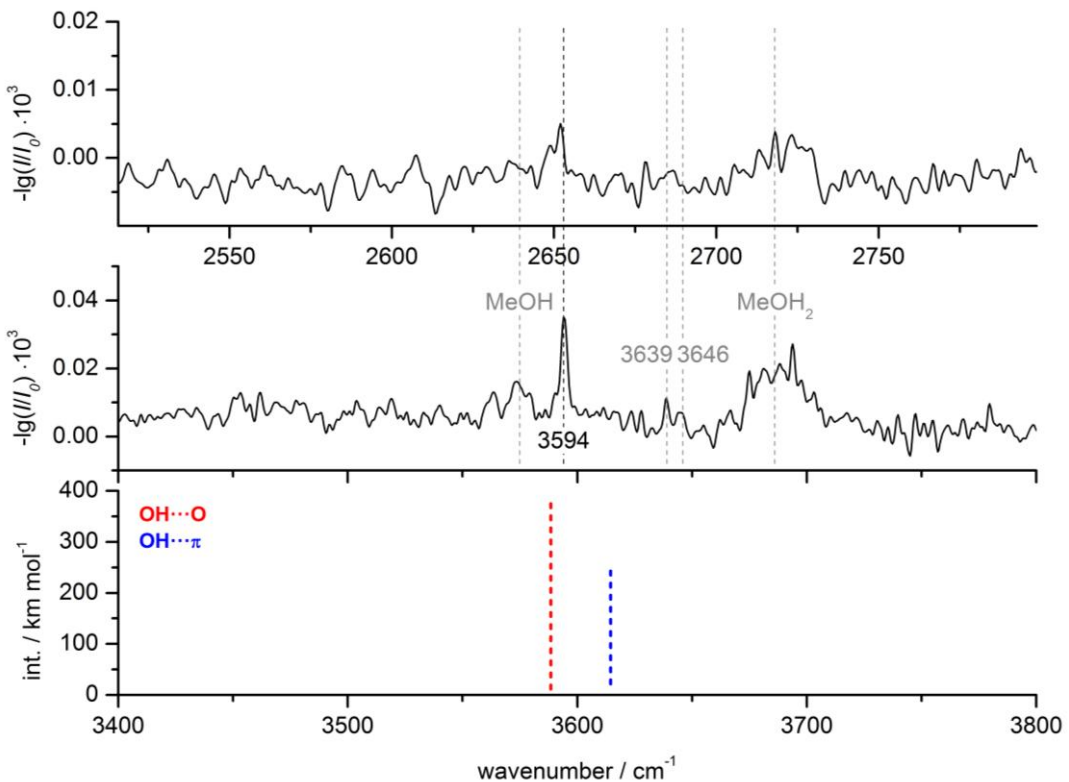


**Fig. S6:** FTIR spectra of DBF–MeOH (middle) and DBF–MeOD (top) in comparison to the predicted (DBF)<sub>2</sub>–MeOH trimer band positions at B3LYP-D3(BJ, abc)/def2-TZVP level. The DBF–MeOH spectrum is identical to spectrum (b) in Figure 3 (main article), the DBF–MeOD spectrum has been measured with identical parameters and aligned in wavenumber to the non-deuterated spectrum by shifting to the MeOH monomer band (+968 cm<sup>-1</sup>) and scaling by a factor of  $\sqrt{2}$ . The predicted frequencies are scaled ( $\times 0.9675$ ) to the methanol monomer OH stretching frequency.

#### Discussion on the trimer band:

The excess of DBF in the expansion hints at a trimer origin of the band at 3594 cm<sup>-1</sup> composed of one methanol and two DBF molecules. This is further supported by the fact that the binding energy for a DBF homodimer is predicted to be larger (38.9 kJ/mol) than for the heterodimer (20.1 kJ/mol) (computed at B3LYP-D3(BJ, abc)/def2-TZVP level using ORCA 4.0 including zero point vibrational energy). Furthermore, the binding for methanol to a DBF dimer (28.4 kJ/mol) is also predicted to be stronger than to a single DBF molecule. Since the red-shift seems large for a cluster containing only one hydrogen bond, some trial structures have been computed at B3LYP-D3(BJ, abc)/def2-TZVP level using ORCA 4.0 (cf. Table S7). Interestingly, an oxygen-bound isomer is favored by 2.0 kJ/mol over the combination of the preferred DBF dimer<sup>6</sup> and DBF–MeOH ( $\pi$ -bound) geometries. The predicted spectral shift (see Fig. S6) is in good agreement, thus the band is tentatively assigned to this oxygen-bound structure, although the predicted shift for the  $\pi$ -bound isomer would also be in agreement.

The assignment to an oxygen-bound cluster is supported by the slightly larger red-shift in the spectrum of DBF–MeOD (see upper panel of Figure S6), when arranging the spectra such that the monomer bands are aligned after stretching the OD region by  $\sqrt{2}$ . It is a signature of larger anharmonicity than in free methanol, which has been observed before for methylated furans.<sup>7</sup> The oxygen-bound dimers similarly showed this larger red-shift, while  $\pi$ -bound clusters were slightly less red-shifted.

**Table S8:** Trial structures for  $(DBF)_2$ -MeOH calculated at B3LYP-D3(BJ, abc)/def2-TZVP level using ORCA 4.0 up to a relative energy of 5 kJ/mol. Relative energies and OH stretching frequencies (scaled to methanol monomer) are also given.

$\Delta E / \text{kJ mol}^{-1}$	0	2.8	2.8	3.3
$\Delta E_0 / \text{kJ mol}^{-1}$	0	2.0	2.3	2.6
$\omega_{\text{OH}} / \text{cm}^{-1}$	3709	3736	3739	3745
$\omega_{\text{OH}} (\times 0.9675) / \text{cm}^{-1}$	3588	3614	3618	3623

**Table S9:** Rotational transitions linelist of DBF-MeOH OH $\cdots$  $\pi$ 6 complex from XIAM.

J'	K <sub>a</sub> '	K <sub>c</sub> '	J''	K <sub>a</sub> ''	K <sub>c</sub> ''	State	v (MHz)	$\Delta v$ (MHz)	
3	0	3	$\leftarrow$	2	1	2	A	2041.3308	-0.0006
3	0	3	$\leftarrow$	2	1	2	E	2041.5279	-0.0012
2	1	2	$\leftarrow$	1	0	1	E	2239.8818	0.0085
2	1	2	$\leftarrow$	1	0	1	A	2240.1024	0.0057
3	1	3	$\leftarrow$	2	1	2	A	2537.7476	0.0017
3	1	3	$\leftarrow$	2	1	2	E	2537.8479	0.0011
3	0	3	$\leftarrow$	2	0	2	A	2568.2214	-0.0011
3	2	2	$\leftarrow$	2	2	1	A	2570.7421	0.0030
3	2	2	$\leftarrow$	2	2	1	E	2571.8466	0.0047
3	2	1	$\leftarrow$	2	2	0	E	2572.1638	0.0022
3	2	1	$\leftarrow$	2	2	0	A	2573.2776	0.0041
3	1	2	$\leftarrow$	2	1	1	E	2602.8606	0.0002
3	1	2	$\leftarrow$	2	1	1	A	2602.9667	0.0017
4	0	4	$\leftarrow$	3	1	3	A	2924.9454	0.0029
4	0	4	$\leftarrow$	3	1	3	E	2925.0219	0.0020
3	1	3	$\leftarrow$	2	0	2	E	3064.5266	0.0015
3	1	3	$\leftarrow$	2	0	2	A	3064.6379	0.0010
4	1	4	$\leftarrow$	3	1	3	A	3382.9531	0.0123
4	0	4	$\leftarrow$	3	0	3	A	3421.3491	-0.0079
4	2	3	$\leftarrow$	3	2	2	A	3427.1553	0.0038
4	2	3	$\leftarrow$	3	2	2	E	3429.0703	0.0007
4	2	2	$\leftarrow$	3	2	1	E	3431.5346	0.0009
4	2	2	$\leftarrow$	3	2	1	A	3433.4672	0.0032
4	1	3	$\leftarrow$	3	1	2	A	3469.8319	-0.0137
4	1	4	$\leftarrow$	3	0	3	A	3879.3570	0.0018
5	1	5	$\leftarrow$	4	1	4	A	4227.5473	-0.0049
5	1	5	$\leftarrow$	4	1	4	E	4227.5874	0.0099
5	2	4	$\leftarrow$	4	2	3	A	4283.1277	-0.0075
5	2	4	$\leftarrow$	4	2	3	E	4284.8867	0.0013
5	4	2	$\leftarrow$	4	4	1	A	4285.8723	0.0013
5	4	1	$\leftarrow$	4	4	0	A	4285.8723	-0.0001
5	3	3	$\leftarrow$	4	3	2	A	4286.5790	0.0069
5	3	3	$\leftarrow$	4	3	2	E	4286.6902	0.0019
5	3	2	$\leftarrow$	4	3	1	E	4286.6902	0.0080
5	3	2	$\leftarrow$	4	3	1	A	4286.8189	0.0038

5	2	3	←	4	2	2	E	4293.9003	0.0023
5	2	3	←	4	2	2	A	4295.6611	-0.0024
5	1	4	←	4	1	3	A	4336.0151	-0.0120
5	1	5	←	4	0	4	A	4685.5463	-0.0042
6	0	6	←	5	1	5	A	4706.3303	-0.0098
6	1	6	←	5	1	5	A	5071.4586	-0.0166
6	0	6	←	5	0	5	A	5119.8233	-0.0200
6	2	5	←	5	2	4	A	5138.5862	0.0022
6	2	5	←	5	2	4	E	5139.5819	0.0013
6	4	3	←	5	4	2	A	5143.4957	0.0032
6	3	4	←	5	3	3	A	5144.5735	0.0043
6	3	4	←	5	3	3	E	5144.8829	0.0028
6	3	3	←	5	3	2	E	5144.8829	-0.0020
6	3	3	←	5	3	2	A	5145.2136	-0.0023
6	2	4	←	5	2	3	E	5159.1999	0.0030
6	2	4	←	5	2	3	A	5160.2157	0.0036
6	1	6	←	5	0	5	A	5484.9764	-0.0019
6	1	6	←	5	0	5	A	5484.9781	-0.0002
6	1	6	←	5	0	5	E	5485.0166	0.0026
6	1	6	←	5	0	5	E	5485.0166	0.0026
8	1	7	←	7	2	6	A	5547.2191	0.0001
7	0	7	←	6	1	6	E	5599.2608	0.0123
7	0	7	←	6	1	6	A	5599.3533	0.0055
7	0	7	←	6	0	6	A	5964.4683	-0.0145
7	2	6	←	6	2	5	A	5993.3913	-0.0019
7	2	6	←	6	2	5	E	5993.8831	-0.0025
7	5	3	←	6	5	2	A	6000.3684	0.0002
7	5	2	←	6	5	1	A	6000.3684	0.0001
7	4	4	←	6	4	3	A	6001.3669	0.0120
7	4	3	←	6	4	2	A	6001.3669	-0.0091
7	3	5	←	6	3	4	A	6002.8473	0.0065
7	3	5	←	6	3	4	E	6003.5164	0.0073
7	3	4	←	6	3	3	E	6003.6062	0.0072
7	3	4	←	6	3	3	A	6004.3002	0.0092
7	2	5	←	6	2	4	E	6026.7331	-0.0122
7	2	5	←	6	2	4	A	6027.2522	-0.0076
7	1	6	←	6	1	5	E	6065.3505	-0.0037
7	1	6	←	6	1	5	A	6065.3910	0.0062
7	1	7	←	6	0	6	A	6279.7669	0.0019
7	1	7	←	6	0	6	E	6279.8494	-0.0060
8	0	8	←	7	1	7	E	6490.5101	0.0047
8	0	8	←	7	1	7	A	6490.6830	0.0044
8	0	8	←	7	0	7	A	6805.9472	-0.0135
8	2	7	←	7	2	6	A	6847.4470	-0.0134
8	2	7	←	7	2	6	E	6847.6942	-0.0148
8	5	4	←	7	5	3	A	6858.0612	-0.0024
8	5	3	←	7	5	2	A	6858.0612	-0.0029
8	4	5	←	7	4	4	A	6859.5005	0.0065
8	3	6	←	7	3	5	A	6861.3547	-0.0021
8	3	6	←	7	3	5	E	6862.5448	-0.0054
8	3	5	←	7	3	4	E	6863.0148	-0.0059
8	3	5	←	7	3	4	A	6864.2469	0.0052
8	1	7	←	7	1	6	E	6927.9849	-0.0086
8	1	7	←	7	1	6	A	6928.0333	0.0056
8	1	8	←	7	0	7	A	7072.2542	0.0076
8	1	8	←	7	0	7	E	7072.4161	0.0055
9	0	9	←	8	1	8	E	7377.9949	0.0035
9	0	9	←	8	1	8	A	7378.2857	0.0162
9	0	9	←	8	0	8	E	7644.4781	-0.0105
9	0	9	←	8	0	8	A	7644.5559	0.0005
9	5	5	←	8	5	4	A	7715.9536	-0.0056
9	3	7	←	8	3	6	A	7720.0643	0.0058

9	3	7	←	8	3	6	E	7721.7923	-0.0011
9	3	6	←	8	3	5	E	7723.5333	-0.0064
9	3	6	←	8	3	5	A	7725.3054	-0.0006
9	2	7	←	8	2	6	E	7767.9552	-0.0048
9	2	7	←	8	2	6	A	7768.1192	-0.0012
9	1	8	←	8	1	7	E	7788.8655	0.0062
9	1	8	←	8	1	7	A	7788.9064	0.0086
9	1	9	←	8	0	8	A	7864.7449	0.0041
9	0	9	←	8	0	8	E	7865.0170	0.0066
RMS								7.1 kHz	

**Table S10:** Rotational transitions linelist of DBF-MeOH OH-Ot complex from AABS program.

J'	K <sub>a</sub> '	K <sub>c</sub> '		J''	K <sub>a</sub> ''	K <sub>c</sub> ''	v (MHz)	Δv (MHz)
3	1	2	←	2	2	1	2036.5750	-0.0065
5	1	4	←	5	0	5	2042.1248	-0.0036
6	4	2	←	6	3	3	2068.9032	-0.0012
4	2	2	←	3	3	1	2261.7426	-0.0103
7	2	5	←	7	1	6	2280.3006	0.0167
5	2	4	←	5	1	5	2284.2879	-0.0124
3	0	3	←	2	1	2	2360.7474	-0.0102
6	3	4	←	6	2	5	2380.4250	0.0034
4	4	0	←	4	3	1	2396.0850	0.0076
4	4	1	←	4	3	2	2454.0398	0.0047
5	4	2	←	5	3	3	2468.5181	0.0010
6	4	3	←	6	3	4	2527.9528	0.0049
5	0	5	←	4	1	3	2550.0674	-0.0050
6	1	5	←	6	0	6	2618.4752	-0.0066
3	1	3	←	2	0	2	2630.9257	0.0038
7	4	4	←	7	3	5	2656.7226	0.0167
6	2	5	←	6	1	6	2737.5694	-0.0079
2	2	1	←	1	1	0	2802.0038	-0.0005
2	2	0	←	1	1	0	2847.1346	-0.0048
7	5	2	←	7	4	3	2923.3241	-0.0109
2	2	0	←	1	1	1	2996.4106	-0.0030
6	3	4	←	5	4	1	2997.6189	-0.0008
6	5	1	←	6	4	2	3058.8104	-0.0025
7	5	3	←	7	4	4	3103.6659	0.0006
4	1	3	←	3	2	2	3115.0674	0.0011
6	5	2	←	6	4	3	3116.2074	0.0116
8	5	4	←	8	4	5	3124.0220	0.0066
5	5	0	←	5	4	1	3126.5646	0.0076
5	5	1	←	5	4	2	3139.1615	0.0057
8	3	6	←	8	2	7	3153.6531	0.0130
7	1	6	←	7	0	7	3170.6431	-0.0079
4	0	4	←	3	1	3	3193.9238	-0.0001
7	2	6	←	7	1	7	3221.8316	-0.0085
4	1	4	←	3	0	3	3321.3985	0.0053
7	4	4	←	6	5	1	3355.4174	0.0094
5	2	3	←	4	3	2	3459.8290	-0.0049
3	1	2	←	2	0	2	3517.5503	-0.0058
6	3	3	←	5	4	2	3529.2117	0.0078
3	2	2	←	2	1	1	3552.5604	-0.0059
8	1	7	←	8	0	8	3702.0100	-0.0143
8	6	2	←	8	5	3	3717.5380	-0.0111
8	2	7	←	8	1	8	3722.1126	-0.0105
3	2	1	←	2	1	1	3756.4081	0.0035
7	3	5	←	6	4	2	3757.5199	0.0049
7	6	1	←	7	5	2	3794.4478	-0.0058
7	6	2	←	7	5	3	3807.4408	-0.0036
6	6	0	←	6	5	1	3836.9007	0.0027

6	6	1	←	6	5	2	3839.2116	0.0040
5	0	5	←	4	1	4	3983.3728	-0.0040
3	2	2	←	2	1	2	4000.3837	-0.0051
8	2	7	←	7	3	5	4025.5725	-0.0029
5	1	5	←	4	0	4	4034.8031	0.0016
5	1	4	←	4	2	3	4143.7136	-0.0007
3	2	1	←	2	1	2	4204.2242	-0.0029
4	2	3	←	3	1	2	4226.5710	0.0041
8	3	6	←	7	4	3	4328.7999	-0.0030
3	3	1	←	2	2	0	4474.2205	0.0023
3	3	1	←	2	2	1	4519.3640	0.0107
3	3	0	←	2	2	1	4528.3666	0.0025
7	7	0	←	7	6	1	4541.7773	-0.0027
7	7	1	←	7	6	2	4542.1655	0.0038
6	2	4	←	5	3	3	4672.2464	0.0092
4	2	2	←	3	1	2	4744.5189	-0.0058
6	0	6	←	5	1	5	4749.7274	0.0005
4	1	3	←	3	0	3	4754.6872	-0.0103
6	1	6	←	5	0	5	4768.4974	0.0019
5	2	4	←	4	1	3	4848.3074	-0.0037
6	1	5	←	5	2	4	5083.9128	0.0043
6	4	2	←	6	1	5	5092.0275	0.0095
9	4	6	←	8	5	3	5108.3521	0.0178
4	2	3	←	3	1	3	5113.1906	-0.0106
4	3	2	←	3	2	1	5284.8212	0.0019
6	2	5	←	5	1	4	5463.9502	0.0058
4	3	2	←	3	2	2	5488.6585	0.0010
7	0	7	←	6	1	6	5506.0484	0.0075
7	1	7	←	6	0	6	5512.4608	-0.0072
4	3	1	←	3	2	2	5548.0927	-0.0021
4	2	2	←	3	1	3	5631.1600	0.0009
5	2	3	←	4	1	3	5833.4365	0.0114
7	2	5	←	6	3	4	5838.9762	-0.0006
7	1	6	←	6	2	5	5939.1183	0.0037
5	3	3	←	4	2	2	5991.1706	0.0029
3	3	0	←	2	0	2	6009.3422	0.0035
5	1	4	←	4	0	4	6062.9835	-0.0080
4	4	1	←	3	3	0	6113.9166	-0.0072
4	4	0	←	3	3	0	6115.4001	-0.0034
7	2	6	←	6	1	5	6115.8206	-0.0057
4	4	1	←	3	3	1	6122.9302	-0.0044
4	4	0	←	3	3	1	6124.4105	-0.0039
5	3	2	←	4	2	2	6201.8801	0.0088
8	0	8	←	7	1	7	6258.4847	-0.0037
8	1	8	←	7	0	7	6260.5988	0.0029
5	2	4	←	4	1	4	6281.6051	-0.0104
5	3	3	←	4	2	3	6509.1405	0.0149
6	3	4	←	5	2	3	6603.1407	-0.0010
5	3	2	←	4	2	3	6719.8327	0.0035
8	1	7	←	7	2	6	6738.6740	0.0013
14	1	13	←	14	0	14	6780.9042	0.0072
8	2	7	←	7	1	6	6812.0827	0.0146
5	4	2	←	4	3	1	6993.0999	-0.0006
5	4	1	←	4	3	1	7005.9149	-0.0035
9	0	9	←	8	1	8	7009.5581	-0.0019
9	1	9	←	8	0	8	7010.2320	0.0024
6	2	4	←	5	1	4	7037.6599	0.0114
5	4	2	←	4	3	2	7052.5398	0.0017
5	4	1	←	4	3	2	7065.3586	0.0026
6	3	3	←	5	2	3	7121.9115	0.0034
7	3	5	←	6	2	4	7151.9024	-0.0007
5	2	3	←	4	1	4	7266.7192	-0.0102

6	1	5	←	5	0	5	7382.1427	-0.0043
6	2	5	←	5	1	5	7492.1286	-0.0058
9	1	8	←	8	2	7	7509.4604	0.0034
9	2	8	←	8	1	7	7537.6288	-0.0141
6	3	4	←	5	2	4	7588.2503	-0.0054
8	3	6	←	7	2	5	7685.4113	-0.0130
5	5	1	←	4	4	0	7736.1861	0.0071
5	5	1	←	4	4	1	7737.6601	0.0013
5	5	0	←	4	4	1	7737.8816	0.0037
10	0	10	←	9	1	9	7760.1554	-0.0073
10	1	10	←	9	0	9	7760.3657	-0.0046
6	4	3	←	5	3	2	7796.1970	-0.0018
6	4	2	←	5	3	2	7855.9270	0.0051
RMS							7.0 kHz	

**Table S11:** Rotational transitions linelist of DBF-*t*-BuOH OH-π6 complex from AABS program.

J'	K <sub>a</sub> '	K <sub>c</sub> '		J''	K <sub>a</sub> ''	K <sub>c</sub> ''	v (MHz)	Δv (MHz)
4	1	4	←	3	1	3	2283.3480	0.0000
4	0	4	←	3	0	3	2313.7664	0.0038
3	1	2	←	2	0	2	2319.7089	0.0041
3	2	1	←	2	1	1	2459.7884	0.0097
4	2	3	←	3	2	2	2466.0297	-0.0068
4	3	2	←	3	3	1	2522.8599	0.0031
4	3	1	←	3	3	0	2549.2883	0.0118
4	1	3	←	3	1	2	2585.6877	-0.0056
4	2	2	←	3	2	1	2636.7963	-0.0055
9	2	8	←	8	3	5	2645.7018	0.0042
3	2	1	←	2	0	2	2810.3783	0.0086
5	1	5	←	4	1	4	2831.2858	0.0009
5	0	5	←	4	0	4	2845.2522	-0.0006
3	3	1	←	2	2	0	2868.5382	0.0080
3	3	0	←	2	2	0	2873.2419	0.0083
3	3	1	←	2	2	1	2892.7650	0.0053
3	3	0	←	2	2	1	2897.4707	0.0076
5	1	4	←	4	2	3	2901.1013	0.0028
5	2	4	←	4	2	3	3053.1668	-0.0010
4	1	3	←	3	0	3	3127.0916	0.0003
4	2	2	←	3	1	2	3127.4743	0.0075
5	3	3	←	4	3	2	3152.8452	-0.0021
5	4	2	←	4	4	1	3160.0613	-0.0038
5	1	4	←	4	1	3	3162.2143	-0.0015
5	4	1	←	4	4	0	3165.8334	-0.0004
5	5	0	←	5	3	3	3175.5720	-0.0039
5	3	2	←	4	3	1	3232.7519	0.0006
5	2	3	←	4	2	2	3308.7229	-0.0037
4	2	3	←	3	1	3	3335.2832	0.0108
6	1	6	←	5	1	5	3374.3304	0.0019
6	0	6	←	5	0	5	3379.8494	-0.0049
4	3	2	←	3	2	1	3441.7534	0.0045
4	3	1	←	3	2	1	3472.8837	0.0117
4	3	2	←	3	2	2	3551.6361	-0.0036
6	2	5	←	5	2	4	3624.9124	-0.0021
3	3	1	←	2	1	2	3625.2590	0.0030
6	1	5	←	5	1	4	3701.6945	-0.0010
6	3	4	←	5	3	3	3772.2361	-0.0113
6	5	2	←	5	5	1	3790.6386	0.0117
6	5	1	←	5	5	0	3791.6756	-0.0003
6	4	3	←	5	4	2	3803.1746	-0.0039
6	4	2	←	5	4	1	3827.1459	-0.0080
5	2	3	←	4	1	3	3850.5074	0.0072

7	3	4	←	7	1	7	3852.9951	0.0077
4	4	1	←	3	3	0	3907.8751	-0.0119
4	4	0	←	3	3	0	3908.6280	-0.0103
4	4	1	←	3	3	1	3912.5769	-0.0134
7	0	7	←	6	1	6	3913.9587	0.0105
7	1	7	←	6	1	6	3914.9743	0.0033
7	0	7	←	6	0	6	3916.9792	0.0032
7	1	7	←	6	0	6	3918.0020	0.0032
6	3	3	←	5	3	2	3936.9436	-0.0002
6	2	4	←	5	2	3	3948.9403	0.0006
4	3	1	←	3	1	2	3963.5507	0.0137
5	1	4	←	4	0	4	3975.5494	0.0047
5	3	2	←	4	2	2	4068.8275	0.0061
7	2	5	←	6	3	4	4073.9215	-0.0052
7	1	6	←	6	2	5	4150.5917	-0.0110
7	2	6	←	6	2	5	4183.4240	-0.0015
7	1	6	←	6	1	5	4225.8955	0.0043
5	3	3	←	4	2	3	4238.4530	0.0024
7	3	5	←	6	3	4	4376.3495	0.0000
6	3	4	←	5	2	3	4421.3276	0.0124
7	5	3	←	6	5	2	4436.7796	-0.0043
7	5	2	←	6	5	1	4442.2589	0.0020
7	4	4	←	6	4	3	4444.3672	-0.0039
8	1	8	←	7	1	7	4454.6088	0.0070
8	0	8	←	7	0	7	4455.2982	0.0079
5	5	1	←	5	1	4	4512.8208	0.0009
7	4	3	←	6	4	2	4513.4902	-0.0005
5	4	1	←	4	3	1	4525.1891	-0.0065
7	2	5	←	6	2	4	4546.2972	-0.0050
5	4	2	←	4	3	2	4549.7917	-0.0069
5	3	2	←	4	1	3	4610.6025	0.0076
7	3	4	←	6	3	3	4635.2330	0.0072
6	3	3	←	5	2	3	4697.0456	0.0070
8	2	7	←	7	2	6	4732.5120	-0.0070
8	1	7	←	7	1	6	4752.2307	-0.0005
8	2	7	←	7	1	6	4765.3309	-0.0109
6	1	5	←	5	0	5	4831.9854	-0.0018
7	3	5	←	6	2	4	4848.7156	-0.0093
6	2	5	←	5	1	5	4898.7264	0.0042
6	3	4	←	5	2	4	4957.5336	0.0034
8	3	6	←	7	3	5	4963.0392	-0.0063
9	1	9	←	8	1	8	4993.8637	0.0113
9	0	9	←	8	0	8	4994.0894	0.0093
8	6	3	←	7	6	2	5065.5943	-0.0011
8	6	2	←	7	6	1	5066.6549	-0.0073
8	4	5	←	7	4	4	5077.3877	-0.0048
8	5	4	←	7	5	3	5086.5702	-0.0022
6	4	3	←	5	3	2	5089.0895	-0.0134
8	2	6	←	7	2	5	5097.7230	0.0026
8	5	3	←	7	5	2	5106.6587	0.0031
6	4	2	←	5	3	2	5119.5863	-0.0119
8	4	4	←	7	4	3	5226.2393	0.0055
6	4	2	←	5	3	3	5230.6181	-0.0071
9	2	8	←	8	2	7	5276.0462	0.0036
9	1	8	←	8	1	7	5284.2261	0.0033
8	3	5	←	7	3	4	5302.7248	-0.0001
7	3	4	←	6	2	4	5383.3242	-0.0004
6	3	3	←	5	1	4	5385.3239	0.0010
7	2	5	←	6	1	5	5481.8347	0.0040
8	8	0	←	8	6	3	5528.5815	0.0010
9	3	7	←	8	3	6	5533.1641	-0.0045
7	4	4	←	6	3	3	5596.5232	-0.0070

9	2	7	←	8	2	6	5619.2787	-0.0047
5	4	2	←	4	2	3	5635.4114	0.0095
5	4	2	←	4	2	3	5635.4114	0.0095
10	7	3	←	10	4	6	5663.1132	0.0046
7	1	6	←	6	0	6	5678.0264	0.0022
7	4	3	←	6	3	3	5696.1301	-0.0150
9	4	6	←	8	4	5	5696.3718	-0.0124
9	3	7	←	8	2	6	5700.9137	-0.0028
7	2	6	←	6	1	6	5707.8230	0.0038
7	3	5	←	6	2	5	5708.9513	-0.0137
9	6	4	←	8	6	3	5716.3914	0.0085
9	6	3	←	8	6	2	5721.0775	0.0108
9	5	5	←	8	5	4	5736.3507	-0.0026
9	5	4	←	8	5	3	5793.1528	0.0132
10	2	9	←	9	2	8	5816.7832	0.0048
10	1	9	←	9	1	8	5819.9356	0.0015
10	2	9	←	9	1	8	5821.7070	-0.0018
7	4	4	←	6	3	4	5872.2506	-0.0030
6	4	2	←	5	2	3	5879.6969	0.0039
9	3	6	←	8	3	5	5925.3676	-0.0076
10	2	8	←	9	2	7	6135.6323	-0.0135
8	3	5	←	7	2	5	6139.7582	0.0107
8	4	4	←	7	3	4	6287.1461	-0.0071
10	4	7	←	9	4	6	6297.5738	-0.0095
10	7	4	←	9	7	3	6343.2052	0.0039
10	7	3	←	9	7	2	6344.1532	-0.0010
8	2	6	←	7	1	6	6353.6508	-0.0090
11	2	10	←	10	2	9	6356.3160	0.0054
11	1	10	←	10	1	9	6357.4724	0.0048
10	6	5	←	9	6	4	6371.3799	0.0031
10	5	6	←	9	5	5	6380.4891	0.0069
6	4	3	←	5	2	4	6385.4173	0.0046
10	6	4	←	9	6	3	6387.4343	0.0045
7	4	3	←	6	2	4	6444.2501	0.0059
8	3	6	←	7	2	6	6488.5764	-0.0086
8	1	7	←	7	0	7	6513.2748	-0.0046
8	4	5	←	7	3	5	6573.2992	0.0024
7	6	1	←	6	5	2	6595.3247	0.0052
11	3	9	←	10	3	8	6637.7589	0.0121
10	4	6	←	9	4	5	6642.4514	0.0133
11	2	9	←	10	2	8	6658.9429	-0.0074
11	4	8	←	10	4	7	6880.1759	-0.0030
9	4	5	←	8	3	5	6930.4496	0.0089
9	3	6	←	8	2	6	6967.3951	-0.0071
11	7	5	←	10	7	4	6997.7250	0.0094
11	7	4	←	10	7	3	7001.5043	0.0003
11	6	6	←	10	6	5	7027.8720	-0.0018
8	4	4	←	7	2	5	7124.1779	0.0022
12	3	10	←	11	3	9	7180.3324	-0.0074
12	2	10	←	11	2	9	7189.3389	-0.0068
7	4	4	←	6	2	5	7204.8523	-0.0169
9	2	7	←	8	1	7	7220.6986	-0.0134
9	4	6	←	8	3	6	7306.6298	-0.0056
9	1	8	←	8	0	8	7342.1979	-0.0140
9	2	8	←	8	1	8	7346.8004	-0.0078
10	4	6	←	9	3	6	7647.5116	0.0080
10	3	7	←	9	2	7	7844.4567	0.0115
							RMS	7.1 kHz

## References

- 1 H. Sasaki, S. Daicho, Y. Yamada, Y. Nibu, *J. Phys. Chem. A*, 2013, **117**, 3183–3189.
- 2 J. Altnöder, A. Bouchet, J. J. Lee, K. E. Otto, M. A. Suhm, A. Zehnacker-Rentien, *Phys. Chem. Chem. Phys.*, 2013, **15**, 10167–10180.
- 3 J. Altnöder, S. Oswald, M. A. Suhm, *J. Phys. Chem. A*, 2014, **118**, 3266–3279.
- 4 A. Poblotzki, J. Altnöder, M. A. Suhm, *Phys. Chem. Chem. Phys.*, 2016, **18**, 27265–27271.
- 5 H. C. Gottschalk, J. Altnöder, M. Heger, M. A. Suhm, *Angew. Chem. Int. Ed.*, 2016, **55**, 1921–1924.
- 6 M. Fatima, A. L. Steber, A. Poblotzki, C. Pérez, S. Zinn, M. Schnell, *Angew. Chem.*, 2019, **131**, 3140–3145.
- 7 H. C. Gottschalk, A. Poblotzki, M. A. Suhm, M. M. Al-Mogren, J. Antony, A. A. Auer, L. Baptista, D. M. Benoit, G. Bistoni, F. Bohle, R. Dahmani, D. Firaha, S. Grimme, A. Hansen, M. E. Harding, M. Hochlaf, C. Holzer, G. Jansen, W. Klopper, W. A. Kopp, L. C. Kröger, K. Leonhard, H. Mouhib, F. Neese, M. N. Pereira, I. S. Ulusoy, A. Wuttke, R. A. Mata, *J. Chem. Phys.*, 2018, **148**, 14301.